

# Experimental Campaign Tests on a Tesla Micro-Expanders

*Avinash Renuke<sup>1,\*</sup>, Alberto Traverso<sup>1</sup>, and Matteo Pascenti<sup>2</sup>*

<sup>1</sup>Thermochemical Power Group (TPG), University of Genoa, Italy

<sup>2</sup>SIT Technologies, Italy

**Abstract.** This paper presents the experimental campaign on Tesla turbo expanders carried out at Thermo-chemical Power group (TPG) of University of Genoa, Italy. An experiment system is established using compressed air as a working fluid. A 200 W turbine is tested with rotational speed up to 40000 rpm. Experimental analysis focused mainly on the efficiency features of this expander, showing the impact on performance of different disk gaps, disk thickness, discharge holes, exhaust geometry, as a function of speed and mass flow. An improved version of 3 kW air Tesla turboexpander is built. Preliminary experimental results are discussed along with the effect of number of nozzles on the performance of the turbine.

## 1 Introduction

In this paper, experimental campaign tests on Tesla micro expanders are described and sample results are reported. This research focuses on investigation of feasibility of Tesla type turbines for micro power generation, thanks to their low cost, simple manufacturing. However, Tesla turbines suffer from poor efficiency. Therefore, this paper focuses on experimental study of a Tesla type micro expander. A flexible test rig is built for a systematic parametric study to understand the sensitivity of different geometric parameters on its performance. In this test campaign, 200 W (M02) Tesla turbine is built, and parametric study is carried out. Based on results and analysis of this turbine, a new 3 kW(M3) turbine fed by air is built and tested.

The bladeless turbomachinery was invented by Nikola Tesla in 1913 [1,2]. Multiple disk turbines consist of an array of parallel thin disks very close to each other, separated by spacers and assembled on a shaft, forming a rotor which is fitted in a cylindrical housing with its ends closed by plates properly fitted with bearings to hold the rotor shaft. Fluid enters tangentially into the turbine from stator. The momentum of the moving fluid is transferred to disks because of viscosity and adhesion. The friction force generated by the fluid transfers this momentum. Many researchers have performed experimental activities on Tesla micro turbines and modified it to enhance its performance. Renuke et al [3] presented a complete analysis of experimental literature in chronological order to understand the progress of research in Tesla turbine domain. Maximum efficiency for air as working fluid is obtained by Rice [4] which is 34.8% with 2.9 kW of power at 17200 rpm.

---

\* Corresponding author: [avinashrenuke@edu.unige.it](mailto:avinashrenuke@edu.unige.it)

## 2 Experimental setups

The Tesla turbines used in the experimental campaign consists of following main components: the rotor, the stator and the casing. The rotor consists of smooth flat disks separated by the spacers. The entire stack of disks and the spacers are held together with the help of bushes. In M02 turbine, the nozzle consists of three different elements with some features in common. As shown in Fig. 1 (d), all the plates have a very large central hole in which rotor is placed with clearance of 0.2 mm. Entire casing with stator plates with rotor inside are held together with twelve small studs. In M3 turbine, nozzle is made up of single piece of metal in which total thickness of nozzle remains the same. Complete stator thickness is equal to that of the pack of disks and spacers in both the models. There are 8 convergent-divergent nozzles used in both the models. In M02 turbine, tests are performed using two adjacent nozzles while in M3 tests are carried out for different number of nozzles.

**Table 1.** Geometrical parameters for both turbine models

Parameters	M02	M3
Outer diameter of disk, mm	64.5	120
Inner diameter of disks, mm	30	60
Number of nozzles	8	8
Gap between disks, mm	0.2	0.1
Disk thickness, mm	0.2	0.1
Number of disks	10	118
Nozzle angle, degree	2.2	2.2
Type of nozzle	Convergent-Divergent	Convergent

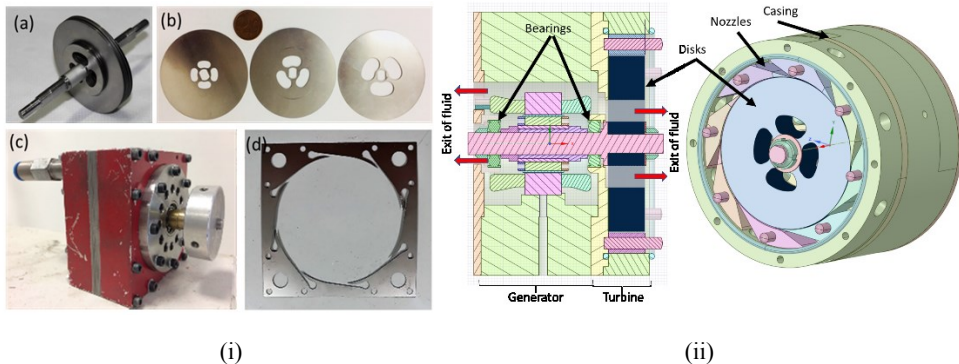


**Fig. 1.** Turbine models: **(i)** M02 turbine with its components - (a) Rotor with disks, spacers and shaft (b) Disks with different central opening (c) Assembled Tesla turbine with flywheel for magnetic braking (d) Stator element; **(ii)** M3 turbine with its components

The first measurement is performed by means of a differential pressure gauge with piezo resistive transducer to measure flow. The temperature measurements are carried out with the help of K-type thermocouples (accuracy of  $\pm 0.5^\circ\text{C}$ ). The first thermocouple (measuring  $T_{line}$ ) is placed after the regulating valve of the air flow. The second (which measures  $T_{in}$ ) is placed at the inlet of turbine. Three thermocouples ( $T_{e1}$ ;  $T_{e2}$ ;  $T_{e3}$ ) are arranged in the exhaust manifold to detect the temperature of the ejected fluid. Speed of rotation of shaft is measured using tachometer which is located at one end of shaft. Pressure (accuracy: 0-7 bar:  $\pm 5\%$ ; 0-1 bar:  $\pm 2.5\%$ ) is measured at different location of turbine: static pressure at the turbine inlet, static pressure in the line, difference in static pressure before and after diaphragm, upstream

of both nozzles and gap between nozzle exit and rotor. The exhaust pressure is not measured by a sensor as the turbine discharge outdoors and is therefore considered the ambient. Torque measurement is carried out using the magnetic eddy current brake coupled to a load cell (accuracy: 0-750g:  $\pm 5$ g). Data is collected using system which consists of microcontroller Arduino [5] which is central processing system. Uncertainty of different measured parameters is considered to calculate the overall uncertainty in the efficiency. Maximum uncertainty in efficiency is found to be  $\pm 0.7\%$  for low mass flow values. To account for the 95.5% confidence interval, standard deviation for all repeated measurements are taken into consideration as  $\pm 2$  SD.

The performance parameters considered for the analysis are as follows: The total pressure and the total temperature at the inlet of the turbine is calculated by:

$$p_{in.tot} = p_{in} + p_{amb} + \frac{\rho_{in} \cdot v^2}{2} \quad (1)$$

$$T_{in.tot} = T_{in} + \frac{v^2}{2c_p} \quad (2)$$

Torque can be directly calculated using the force measured by the load cell,  $Fr$  and arm of the flywheel  $l$ ,

$$\tau = Fr \cdot l \quad (3)$$

It is therefore possible to calculate the mechanical power using torque of the rotor and angular velocity as:

$$P_{exp} = \tau \cdot \omega \quad (4)$$

Mechanical efficiency of total-to-static  $\eta_{exp.tot.st}$ , computed as the ratio of actual enthalpy drop to the isentropic enthalpy drop across turbine. Isentropic expansion of air at lower pressures does not produce very high temperature drop. Uncertainty in measuring temperature is  $\pm 0.5^\circ$  C which gives more uncertainty in the measurement of efficiency. Measuring torque of the turbine gives very less uncertainty compared to enthalpy estimation from temperature. Efficiency evaluation using measured torque is done in this paper due lower uncertainty.

$$\eta_{exp.tot.st} = \frac{h_{in} - h_e}{h_{in} - h'_e} \quad (5)$$

$$\eta_{exp.tot.st} = \frac{P_{exp}}{c_p T_{in.tot} \left( 1 - \frac{1}{\varepsilon^{\frac{k-1}{k}}} \right) \dot{m}} \quad (6)$$

Specific heat at constant pressure,  $C_p$  and heat capacity ratio,  $k$  is considered constant with temperature. For air,  $C_p = 1.005$  kJ/kg.K and  $k = 1.4$  is used.

The parameter expansion ratio  $\varepsilon$  is given by,

$$\varepsilon = \frac{p_{in.tot}}{p_{e.st}} \quad (7)$$

### 3 Results

This section presents the results and the discussion for the tests performed on both the turbines i.e. M02 and M3.

#### 3.1 Turbine M02

In this section, test results for different configuration according to Table 2 are discussed. All tests shown here are performed with two subsequent nozzles, out of 8 total nozzles available.

**Table 2.** Different configuration of parameters for experimental study

Disk Thickness [mm]	Gap [mm]	Disk inner diameter [mm]	Exhaust area [mm <sup>2</sup> ]	Number of disks
<b>Effect of gap between disks</b>				
0.1	<b>0.1</b>	25	A2	20
0.1	<b>0.2</b>	25	A2	14
0.1	<b>0.3</b>	25	A2	11
<b>Effect of disk thickness</b>				
<b>0.3</b>	0.2	25	A2	8
<b>0.2</b>	0.2	25	A2	10
<b>0.1</b>	0.2	25	A2	14
<b>Effect of disk inner diameter</b>				
0.3	0.2	<b>20</b>	A2	10
0.3	0.2	<b>25</b>	A2	10
0.3	0.2	<b>30</b>	A2	10
<b>Effect of exhaust area</b>				
0.2	0.2	25	<b>A1</b>	10
0.2	0.2	25	<b>A2</b>	10

Tests are carried out for three different disk thicknesses. In Fig. 2, at lower rotational speed and low flow, effect of disk thickness is not significant on the performance of the turbine but at higher flow disk thickness plays an important role. If we compare results at different rotational speeds, at higher rotational speed disk thickness should be as small as possible. If disk thickness would be zero, entire flow out of the nozzle would see the same cross section at rotor inlet. In this case we would not expect any major change in the velocity of the fluid. However, when disk thickness is finite, flow area at the rotor inlet decreases which changes the inlet velocity at the rotor. At higher rotational speed and high mass flow, fluid velocity is high. Contraction of area due to finite disk thickness creates losses. This explains the sensitivity of disk thickness at higher mass flow and higher rotational speeds.

Radius ratio of a disk is varied by fixing the outer diameter and changing inner diameter of disks. There are three inner diameters for which tests are performed. We can see in Fig.3, variation of Total to static efficiency with respect to mass flow for two different speeds. It has been observed that small inner diameters are performing better at lower speeds (< 25000 rpm) and medium diameter configuration till 30000 rpm. Although there is an optimum value for inner disk diameter, the dependence on efficiency on inner disk diameter is weak.

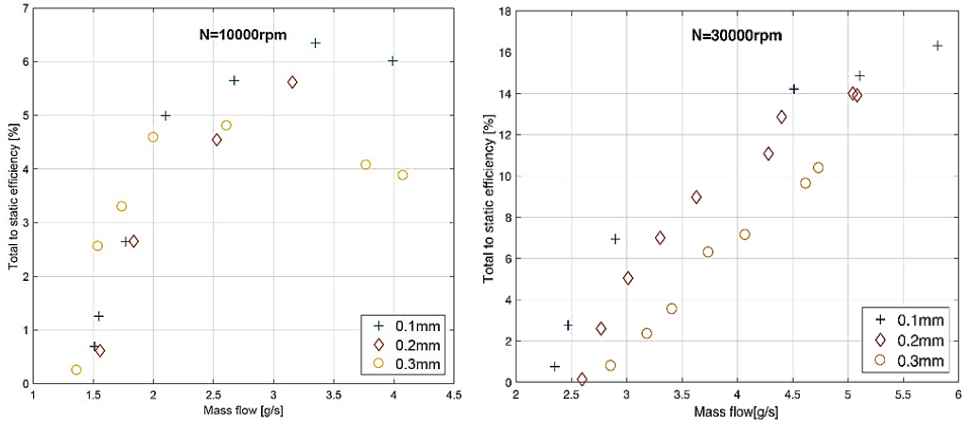


**Fig. 2.** Variation of Total to static efficiency vs mass flow for different thickness of disks at 10000 and 30000 rpm

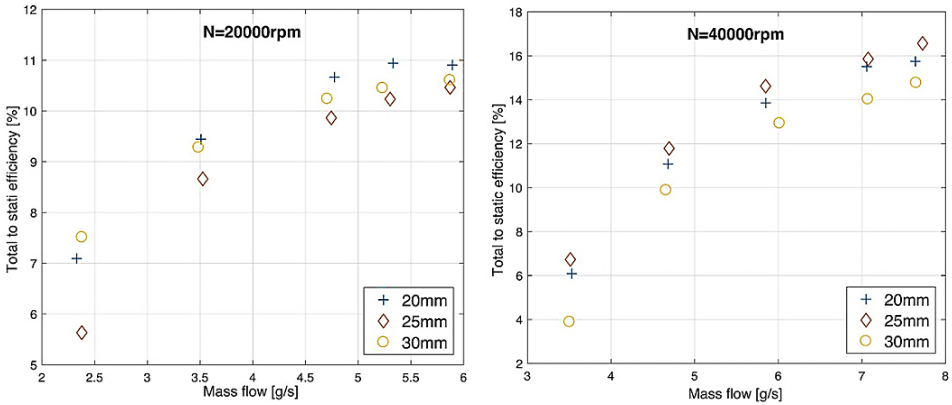


**Fig. 3.** Variation of Total to static efficiency vs mass flow for different inner diameter at 20000 and 40000 rpm.

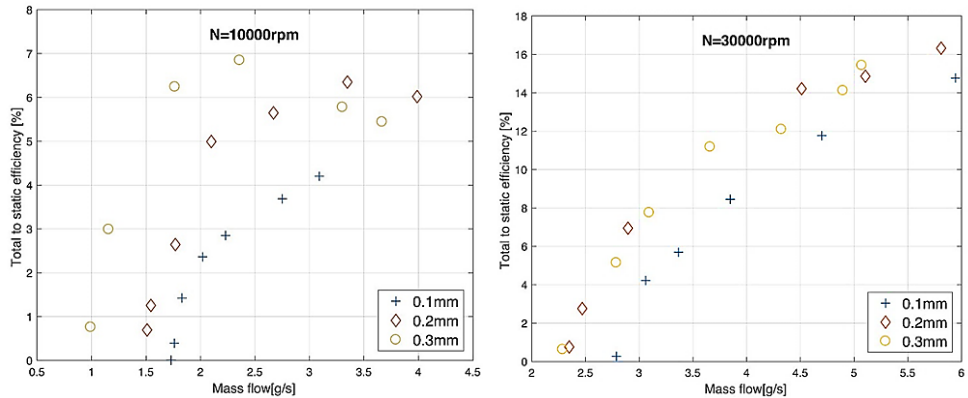


**Fig. 4.** Variation of Total to static efficiency vs mass flow for different gap between disks at 10000 and 30000 rpm

Gap between disks is one of the most important geometric parameters in the performance of the Tesla turbine. Tests are carried out for three different disks spacing. Results show that there is optimum value of the gap width for different speeds of the turbine and specific inlet conditions. In Fig. 4, we can see that when gap between disks is high, 0.3 mm, for lower rotational speed, at same mass flow, performance of the turbine is better. While at higher mass flow efficiency decreases compared to higher rotational speed. Gap width affects the leakage around the end walls based on pressure drop across rotor. For lower gap, pressure drop across rotor will be higher and hence more flow will bypass the rotor leading to lower performance. This can be the reason why 0.1 mm gap between disks shows lower efficiency. However, there is an optimum gap which depends on both rotational speed and mass flow rate of the turbine.

Turbine is also tested for different exhaust areas A1 and A2 where  $A2 > A1$ . Fig. 5 (i) shows that exhaust area has significant impact on the performance of the turbine.

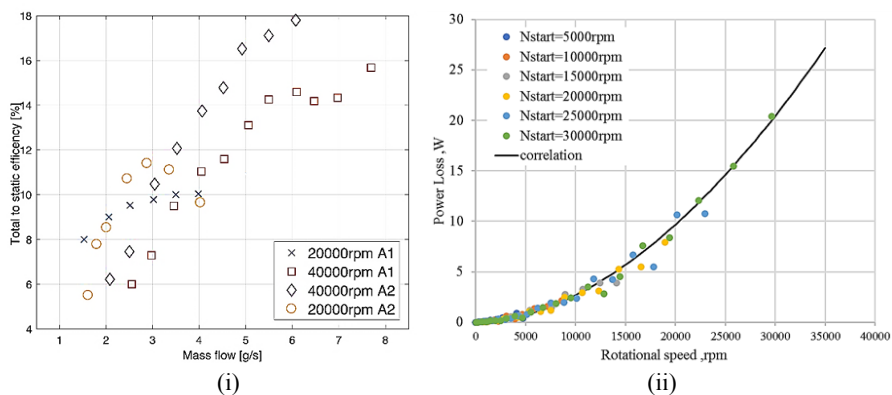
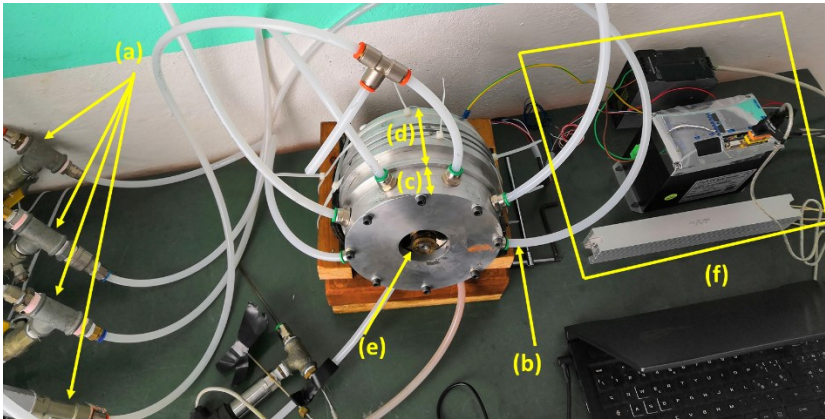


**Fig. 5. (i)** Variation of Total to static efficiency vs mass flow for different exhaust area A1 and A2 for two different speeds where  $A2 > A1$ ; **(ii)** Ventilation loss as a function of rotor speed

Ventilation loss which consists of friction loss between disk tip and the top wall of the casing, friction loss between side wall of the casing and the last disks of the rotor and bearing losses. These losses are estimated by performing a run-down test. A run-down test is performed by switching off the supply of air when turbine is running at desired speed. Due to frictional forces and resistance from the ventilation fluid, and bearing friction, rotor decelerates. This complete deceleration of the rotor in the form of rotor speed and time is recorded. The resistive torque is then calculated by numerically differentiating angular velocity to obtain angular acceleration and multiplying it with moment of inertia of rotor. Fig 5 (ii) shows the power loss due ventilation at different rotational speeds, demonstrating consistency and acceptable repeatability.

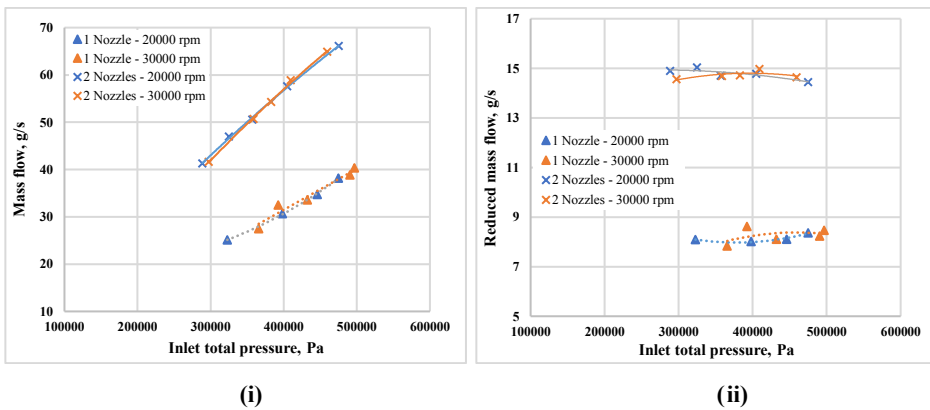
### 3.2 Turbine M3

In this section, preliminary test results for M3 turbine are presented. Figure 6 shows the experimental setup for M3 turbine and generator. Eight flow control valves feed the compressed air to 8 nozzles distinctly. Air flow through each nozzle can be controlled using these flow control valves. High speed permanent magnet generator and turbine are connected in a single casing to make equipment compact. Both the exhausts of the turbine are exposed to ambient – one of them passes over generator stator for cooling. Power generated by the turbine is dissipated as DC current through a resistor.



**Fig. 6.** M3 turbine test setup: (a) Flow valve control for 8 nozzles; (b) Inlet connection to nozzles; (c) Turbine; (d) Generator; (e) Turbine exhaust (on both sides); (f) Generator driver, power conditioner and data acquisition system

Figure 7 (i) shows the preliminary results of the test performed to partially characterize nozzle behaviour. The design point of the turbine is at the 66 g/s mass flow at 30000 rpm with 2.41 bar nozzle inlet pressure corresponding to 8 nozzles. The current test for the turbine is carried out by operating one nozzle and two opposite nozzles to assess the effect of number of nozzles on the performance of turbine. Individual compressed air lines for each nozzle which ensure that each nozzle sees same inlet total pressure. Hence, one nozzle configuration, for same inlet pressure, will have half the mass flow compared to total mass flow of two nozzles configuration which can also be inferred in Fig 7(i).



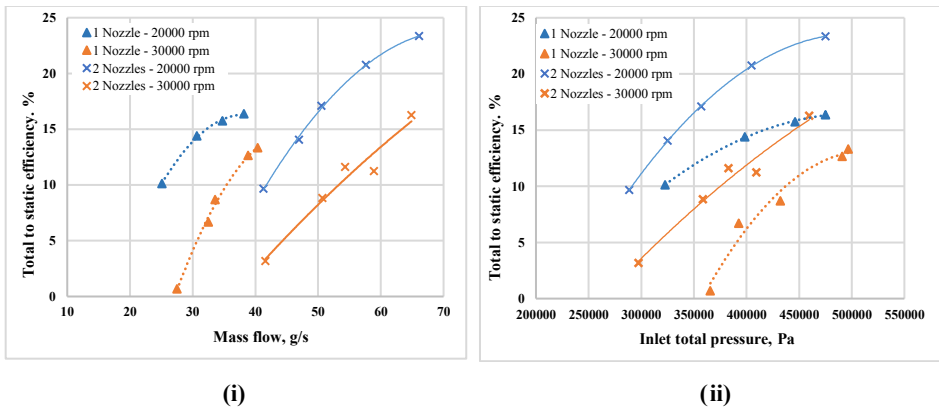
**Fig. 7.** Preliminary test results for M3 turbine: (i) Variation of mass flow versus total inlet pressure at different number of nozzles and different rotational speeds; (ii) Variation of reduced mass flow through turbine versus nozzle inlet total pressure.

Figure 7 (ii) shows the variation of reduced mass flow through turbine versus nozzle inlet total pressure. The reduced flow is calculated at reference temperature and pressure of 288.15 K and 101325 Pa respectively using following equation:

$$\dot{m}_{RID} = \frac{\dot{m} \cdot \sqrt{\frac{T_{in}}{T_{rif}}}}{p_{in}/p_{rif}} \quad (8)$$

where  $T_{in}$  and  $p_{in}$  are inlet total temperature and pressure.

The reduced mass flow rate is almost constant with increasing inlet pressure which indicates that nozzle is choked. Turbine could not generate enough power at low mass flow rates to overcome losses. Hence the performance at low mass flow has not been reported. Figure 8 shows the performance of the turbine in terms of total to static efficiency with mass flow and inlet total pressure. We observe that turbine shows higher performance at lower rotational speeds for both single and two nozzle configurations for same inlet pressure and same total mass flow. This might be due to higher ventilation and bearing losses at higher



**Fig. 8.** Preliminary test results for M3 turbine: (i) Variation of total to static efficiency versus mass flow at different number of nozzles and different rotational speeds; (ii) Variation of total to static efficiency versus total inlet pressure at different number of nozzles and different rotational speeds

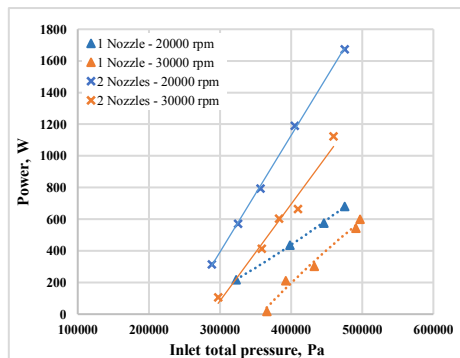


**Fig. 9.** Preliminary test results for M3 turbine: variation of mechanical power versus total inlet pressure at different number of nozzles and different rotational speeds;

rotational speeds. This can be seen in Fig. 9 where power produced by two nozzles at the same inlet pressure is more than double with respect to single nozzle. We have seen in Fig 5 (ii) that ventilation losses increase with rotational speed. These losses seem to have a larger relative impact at low mass flow rates and decrease at higher flow rates as seen for single



nozzle configuration in Fig. 8. However, for two nozzle configuration influence of ventilation loss on mass flow variation is minimal as inferred in Fig.8 (i). Ventilation losses are relatively insensitive to the number of nozzles. In case two nozzles are operated, net power is increased and their impact on efficiency is lower.

Figure 8 also shows the effect of number of nozzles on the performance of turbine. In this paper the preliminary tests only for two cases are presented: single nozzle and two nozzles. We observe that efficiency of the turbine is higher when higher number of nozzles are used for same inlet pressure. Higher the number of nozzles, more uniform flow entry/distribution around the circumference of the disks. The rotor efficiency is maximum when flow is uniformly distributed around the periphery. Hence it is advised to use higher number of nozzles, for fixed inlet pressure, for better performance of the Tesla turbine. This is very significant information coming out of this test as this behavior has never been studied either experimentally or numerically in the past.

The best efficiency point for M3 turbine obtained from 3D computational fluid dynamics analysis is at design values: 2.4 bar inlet pressure at 30000 rpm [6]. This turbine currently has not been tested at its full capacity and for higher number of nozzles. Current performance results are for off design cases. However, turbine shows significant improvement in the performance over M02 turbine. In the next phase of the test campaign we plan to perform the test on M3 turbine at design point at higher number of nozzles and characterize the losses experimentally reaching the 3kW rated power.

## 4 Conclusions

This paper summarizes experimental campaign tests for Tesla micro expanders for 200 W (M02) and 3 kW (M3) design power. Experimental analysis of M02 turbine focused mainly on the efficiency features, showing the impact on performance of different disk gaps, disk thickness, discharge holes, exhaust geometry, as a function of speed and mass flow. A maximum adiabatic efficiency of 18% has been measured, with many other points in the 10-15% range. Preliminary tests for M3 turbine have been presented with partial characterization of nozzles. Two nozzles configuration shows significant improvement of performance of the turbine over single nozzle case for the same nozzle inlet pressure condition. The maximum efficiency of 23% is obtained with two nozzles at 20000 rpm.

This project has received funding from the European Union's Horizon 2020 research and innovation programme under grant agreement No 764706, PUMP-HEAT.

## References

1. Tesla, N., 1913, "Turbine", US Patent 1061206.
2. Tesla, N., 1913, "Fluid propulsion", US Patent 1061142.
3. Renuke, A., Vannoni, A., Traverso, A., and Pascenti, M., 2019, "Experimental Investigation of Tesla Micro Expanders", *Proceedings: ASME TurboExpo '19*, Phoenix, GT2019-91352, USA
4. Rice, W., 1965, "An Analytical and Experimental Investigation of Multiple Disk Turbines", *Journal of Engineering for Power*, Vol. 87(1), pp. 29–36.
5. Arduino hardware, <https://www.arduino.cc/>, last access 01/11/2018
6. Renuke, A., Traverso, A., and Pascenti, M., "Performance Assessment of Bladeless Micro-Expanders Using 3D Numerical Simulation", *Proceeding: SUPEHR'19*, 2019